

ENGINEERING SEISMOLOGY

Julian J. Bommer, Department of Civil and Environmental Engineering, Imperial College London, London SW7 2AZ, United Kingdom.

David M. Boore, US Geological Survey, Menlo Park, CA 94025, USA.

INTRODUCTION

Engineering Seismology is an integral part of Earthquake Engineering, a specialised branch of civil engineering concerned with the protection of the built environment against the potentially destructive effects of earthquakes. The objective of earthquake engineering can be stated as the reduction or mitigation of seismic risk, which is understood as the possibilities of losses – human, social or economic – being caused by earthquakes. Seismic risk exists because of the convolution of three factors: seismic hazard, exposure and vulnerability. Seismic hazard refers to the effects of earthquakes that can cause damage in the built environment, such as the primary effects of ground shaking or ground rupture or secondary effects such as soil liquefaction or landslides. Exposure refers to the population, buildings, installations and infrastructure encountered at the location where earthquake effects could occur. Vulnerability represents the likelihood of damage being sustained by a structure when exposed to a particular earthquake effect.

EARTHQUAKE HAZARDS AND SEISMIC RISK

Risk can be reduced in two main ways, the first being to avoid exposure where seismic hazard is high. However, human settlement, the construction of industrial facilities and the routing of lifelines such as roads, bridges, pipelines, telecommunications and energy distribution systems are often governed by other factors that are of greater importance. Indeed, for lifelines, which may have total lengths of hundreds of kilometres, it will often be impossible to avoid seismic hazards by re-location. Millions of people are living in areas of the world where there is appreciable seismic hazard. The key to mitigating seismic risk therefore lies in control of vulnerability in the built environment, by designing and building structures and facilities with sufficient resistance to withstand the effects of earthquakes; this is the essence of Earthquake Engineering.

This is not to say, however, that the aim is to construct an earthquake-proof built environment that will suffer no damage in the case of a strong earthquake. The cost of such levels of protection would be extremely high, and moreover it might mean protecting the built environment against events that may not occur within the useful life of a particular building. It is generally not possible to justify such investments, especially

when there are many competing demands on resources. Objectives of earthquake-resistant design are often stated in terms that relate different performance objectives to different levels of earthquake motion, such as no damage being sustained due to mild levels of shaking that may occur frequently, damage being limited to non-structural elements or to easily repairable levels in structural elements in moderate shaking that occurs occasionally, and collapse being avoided under severe ground shaking that is only expected to occur rarely. These objectives are adjusted according to the consequences of damage to the structure; for rare occurrences of intense shaking, the performance target for a single-family dwelling will be to avoid collapse of structural elements, so that the occupants may escape from the building without injury. For a hospital or fire station the performance target will be to remain fully operational under the same level of shaking, since the services provided will be particularly important in the aftermath of an earthquake. For a nuclear power plant or radioactive waste repository, the performance objective will be to maintain structural integrity even under extreme levels of shaking that may be expected to occur very rarely.

Once planners and developers have taken decisions regarding the location of civil engineering projects, or once people have begun to settle in an area, the level of exposure is determined. In general, seismic hazard cannot be altered, whence the key to mitigating seismic risk levels lies in the reduction of vulnerability, or stated another way, through the provision of earthquake resistance. In order to provide effective earthquake protection, the civil engineer requires quantitative information on the nature and likelihood of the expected earthquake hazards. As indicated above, this may mean defining the hazard not in terms of the effects a single earthquake event may produce at the site, but a synthesis of the potential effects of many possible earthquake scenarios and quantitative definitions of the particular effects that may be expected to occur with different specified frequencies. This is the essence of Engineering Seismology: to provide quantitative assessments of earthquake hazards.

Earthquake generation creates a number of effects that are potentially threatening to the built environment (**Figure 1**). These effects are earthquake hazards and Engineering Seismology, in the broadest sense, is concerned with assessing the likelihood and characteristics of each of these hazards and their possible impact in a given region or at a given site of interest. Earthquakes are caused by sudden rupture on geological faults, the slip on the fault rupture ranging from a few centimetres for moderate earthquakes (magnitudes from 5 to about 6½) to many metres for large events. In those cases where the fault extends to the ground surface (which is often not the case), the relative displacement of the two sides of the fault present an obvious hazard to any structure crossing the fault trace. In the 17 August 1999 Kocaeli earthquake in Turkey, several hundred houses and at least one industrial facility were severely damaged by the surface deformations associated with the slip on the North Anatolian fault. However, buildings must be situated within a few metres of the fault trace for surface rupture to be a hazard, whereas ground shaking effects can present a serious hazard even at tens of kilometres from the fault trace; hence even if the fault

rupture is tens or even hundreds of kilometres in length, the relative importance of surface rupture hazard is low. An exception to this is where lifelines, particularly pipelines, cross fault traces, although identification and quantification of the hazard allows design to take into account the expected slip in the event of an earthquake: in the vicinity of the Denali fault, the trans-Alaskan oil pipeline is mounted on sleepers that allow lateral movement, which permitted the pipeline to remain functional despite more than 4 m of lateral displacement on the fault in the magnitude 7.9 earthquake of 3 November 2002.

Surface fault ruptures in the ocean floor can give rise to tsunamis, seismic sea waves generated by the sudden displacement of the surface of the sea that travel with very high speeds. As the waves approach the shore and the water depth decreases, the amplitude of the waves increases to maintain the momentum, reaching heights of up to 30 m. As the waves impact on low lying coastal areas, the destruction can be almost total.

All the other hazards generated by earthquakes are directly related to the shaking of the ground caused by the passage of seismic waves. The rapid movement of building foundations during an earthquake generates inertial loads that can lead to damage and collapse, which is the cause of the vast majority of fatalities due to earthquakes. For this reason, the main focus of Engineering Seismology, and also of this chapter, is the assessment of the hazard of ground shaking. Earthquake ground motion can be amplified by features of the natural environment, increasing the hazard to the built environment. Topographic features such as ridges can cause amplification of the shaking, and soft soil deposits also tend to increase the amplitude of the shaking with respect to rock sites. At the same time, the shaking can induce secondary geotechnical hazards by causing failure of the ground. In mountainous or hilly areas, earthquakes frequently trigger landslides, which can significantly compound the losses: the 6 March 1987 earthquake in Ecuador triggered landslides that interrupted a 40 km segment of the pipeline carrying oil from the production fields in the Amazon basin to the coast, thereby cutting one of the major exports of the country; the earthquake that struck El Salvador on 13 January 2001 killed about 850 people, nearly all of them buried by landslides. In areas where saturated sandy soils are encountered, the ground shaking can induce liquefaction through the generation of high pore water pressures leading to reduced effective stress and a significant loss of shear strength, which in turns leads to the sinking of buildings into the ground and lateral spreading on river banks and along coasts. Extensive damage in the 17 January 1994 Kobe earthquake was caused by liquefaction of reclaimed land, leaving Japan's second port out of operation for three years.

The assessment of landslide and liquefaction hazard involves evaluating the susceptibility of slopes and soil deposits, and determining the expected level of earthquake ground motion. The basis for earthquake-resistant design of buildings and bridges also requires quantitative assessment of the ground motion that may be

expected at the location of the project during its design life. Seismic hazard assessment in terms of strong ground-motion is the activity that defines Engineering Seismology.

MEASURING EARTHQUAKE GROUND-MOTION

The measurement of seismic waves is fundamental to seismology. Earthquake locations and magnitudes are determined from recordings on sensitive instruments (called seismographs) installed throughout the world, detecting imperceptible motions of waves generated by events occurring hundreds or even thousands of kilometres away. Engineering Seismology deals with ground motions sufficiently close to the causative rupture to be strong enough to present a threat to engineering structures. There are cases where destructive motions have occurred at significant distances from the earthquake source, generally as the result of amplification of the motions by very soft soil deposits, such as in the San Francisco Marina District during the 18 October 1989 Loma Prieta earthquake, and even more spectacularly in Mexico City during the 19 September 1985 Michoacan earthquake, almost 400 km from the earthquake source. In general, however, the realm of interest of Engineering Seismology is limited to a few tens of kilometres from the earthquake source, perhaps extending 100 km or a little more for the largest magnitude events.

Seismographs specifically designed for measuring the strong ground-motion near to the source of earthquakes are called accelerographs, and the records that they produce are accelerograms. The first accelerographs were installed in California in 1932, almost four decades after the first seismographs, the delay being caused by the challenge of constructing instruments that were simultaneously sensitive enough to produce accurate records of the ground acceleration whilst being of sufficient robustness to withstand the shaking without damage.

Prior to the development of the first accelerographs the only way to quantify earthquake shaking was through the use of intensity scales, which provide an index reflecting the strength of ground shaking in a particular location during an earthquake. The index is evaluated on the basis of observations of how people, objects and buildings respond to the shaking (**Table 1**). Some intensity scales also include the response of the ground with indicators such as slumping, ground cracking and landslides, but these phenomena are generally considered to be dependent on too many variables to be reliable indicators of the strength of ground shaking. At the lower intensity degrees, the most important indicators are related to human perception of the shaking, whereas at the higher levels the assessment is based primarily on the damages sustained by different classes of buildings. A common misconception is that intensity is a measure of damage, whereas it is in fact a measure of the strength of ground motion inferred from building damage, whence a single intensity degree can correspond to severe damage in vulnerable rural dwellings and minor damage in engineered constructions. The most widely used intensity scales, both of which have 12 degrees and which are broadly equivalent, are the Modified Mercalli (MM), used in the Americas, and the European

Macroseismic Scale (EMS-98), which has replaced the Medvedev-Sponheuer-Karnik (MSK) scale.

A very useful picture of the strength and distribution of ground shaking in an earthquake can be obtained by mapping intensity observations. The modal value is assigned to each given location, such as a village, from all the individual point observations gathered, and then lines called isoseismals are drawn to enclose areas where the intensity reached the same degree (**Figure 2**). Such isoseismal maps have many applications, one of the most important of which is to establish correlations between earthquake size (magnitude) and the area enclosed by isoseismals. These empirical relations can then be used to estimate the magnitude of historical earthquakes that occurred before the advent of the global seismograph network at the end of nineteenth century but for which it is possible to compile isoseismal maps from written accounts of the earthquake effects. For engineering design and analysis, however, intensity values are of limited use since they cannot be reliably translated into numerical values related to the acceleration or displacement of the ground. Indeed, intensities are usually expressed in Roman numerals precisely to reinforce the idea that they are broad indices rather than numerical measurements. This is why accelerograms are invaluable to earthquake engineering, providing detailed measurements of the actual movement of the ground during strong earthquake-induced shaking.

Accelerograms generally consist of three mutually perpendicular components of motion, two horizontal and one vertical, registering the ground acceleration against time (**Figure 3**). The first generation of accelerographs produced analogue records on paper or film, which had to be digitised in order to be able to perform numerical analyses. The analogue recording and the digitisation process both introduce noise into the signal that then requires processing of the time-series to improve the signal-to-noise ratio, particularly at long-periods. This processing generally involves the application of digital filters. The current generation of accelerographs record digitally, thus by-passing the time-consuming and troublesome process of digitisation and producing records with much lower noise contamination. Another advantage of digital accelerographs is that they record continuously on re-usable media, whereas optical-mechanical instruments remained on stand-by until triggered by a minimum threshold acceleration, thus missing the very first wave arrivals. Although the motions missed by an analogue instrument are generally very small, the advantage with a digital record is that the boundary conditions of initial velocity and displacement are known with greater confidence; the time-series of velocity and displacement are obtained by simply double integrating the acceleration over time (**Figure 4**).

CHARACTERISING STRONG GROUND-MOTION

A number of parameters are used to characterise the nature of the earthquake ground-motion captured on an accelerogram, although in isolation none of them is able to fully

represent all of the important features. The simplest and most widely used parameter is the peak ground acceleration (PGA), which is simply the largest absolute value of acceleration in the time-series; the horizontal PGA is generally treated separately from the peak vertical motion. Similarly the peak values of velocity (PGV) and displacement (PGD) are also used to characterise the motion, although the latter is difficult to determine reliably from an accelerogram because of the influence of the unknown baseline on the records and the double-integration of the long-period noise in the record. These parameters are particularly poor for characterising the overall nature of the motion since they only reflect the amplitude of a single isolated peak (**Figure 5**). In Engineering Seismology, unlike geophysics, accelerations are generally expressed in units of g , the acceleration due to gravity (9.81 m.s^{-2}).

Another important characteristic of the ground motion is the duration of shaking, particularly of the portion of the accelerogram where the motion is intense. There are many different ways in which the duration of the motion can be measured from an accelerogram, one of the more commonly used definitions being the total interval between the first and last excursions of a specified threshold, such as $0.05g$. Duration of shaking is particularly important in the assessment of liquefaction hazard since the build-up of pore water pressures is controlled by the duration of shaking for motions as well as the amplitude of the motions.

A parameter that measures the energy content of the ground shaking is the Arias intensity, which is the integral over time of the square of the acceleration. A plot of the build-up of Arias intensity with time is known as a Husid plot (**Figure 6**) and it serves to identify the interval over which the majority of the energy is imparted. The root-mean-square acceleration (a_{rms}) is the equivalent constant level of acceleration over any specified interval of the accelerogram; the a_{rms} is also the square root of the gradient of the Husid plot over the same interval. Arias intensity has been found to be a useful parameter to define thresholds of shaking that trigger landslides.

For engineering purposes, the most important representation of earthquake ground-motion is the response spectrum, which is a graph of the maximum response experienced by a series of single-degree-of-freedom (SDOF) oscillators when subjected to the acceleration time-series at their bases (**Figure 7**). The dynamic characteristics of a SDOF system, such as an idealised inverted pendulum, are fully described by its natural period of free vibration and its damping, usually modelled as an equivalent viscous damping and expressed as a proportion of the critical damping that returns a displaced SDOF system to rest without vibrations. In earthquake engineering, the default value generally used is 5% of critical damping, the nominal level of damping in a reinforced concrete structure. The response can be measured in terms of the absolute acceleration of the mass of the system, or in terms of its velocity or displacement relative to the base. The most widely used spectrum currently is the acceleration response, because the acceleration at the natural period of the structure can be multiplied by the mass of the building to estimate the lateral force exerted on the

structure by the earthquake shaking. The natural period of vibration of a building can be very approximately estimated, in seconds, as the number of storeys divided by ten. The acceleration response spectrum intersects the vertical axis at PGA (**Figure 8**). PGA as a ground-motion parameter has many shortcomings, including a very poor correlation with structural damage, but one of the main reasons for its persisting use is the fact that it is essentially defines the anchor point for the acceleration response spectrum. The relationship between the natural period of vibration of the building and the frequency content of the ground motion is a critical factor in determining the impact of earthquake shaking on buildings.

In recent years there has been a gradual tendency to move away from the use of acceleration response spectra in force-based seismic design towards displacement-based approaches, since structural damage is much more closely related to displacements than to the forces that are imposed on to buildings very briefly during ground shaking. Techniques for assessing the seismic capacity of existing buildings have already adopted displacement-based approaches, giving rise to greater interest in displacement response spectra (**Figure 9**).

PREDICTION OF EARTHQUAKE GROUND MOTION

Recordings of ground motions in previous earthquakes are used to derive empirical equations that may be used to estimate values of particular ground-motion parameters for future earthquake scenarios. Such empirical equations have been derived for a variety of parameters but the most abundant are those for predicting PGA and ordinates of acceleration response spectra. The equations are often referred to as attenuation relationships but this is a misnomer because the equations describe both the attenuation (decay) of the amplitudes with distance from the earthquake source and the scaling (increase) of the amplitudes with earthquake magnitude. These two parameters, earthquake magnitude and source-to-site distance, are always included in ground-motion prediction equations (**Figure 10**). The equations are simple models for a very complex phenomenon and as such there is generally a large amount of scatter about the fitted curve (**Figure 11**). The residuals of the logarithmic values of the observed data points are generally found to follow a normal or Gaussian distribution about the mean and hence the scatter can be measured by the standard deviation. Predictions of PGA at the 84-percentile level (i.e. one standard deviation above the mean value) will generally be as much as 80% higher than the median predictions (**Figure 12**).

The nature of the surface geology can also exert a pronounced effect on the recorded ground motion. The presence of soft soil deposits of more than a few metres thickness will tend to amplify the ground motion as the waves propagate from the stiffer materials below to the surface (**Figures 2b, 13**). To account for this effect, site classification is generally included as a third explanatory variable in prediction equations for response spectrum ordinates, allowing spectra to be predicted for a different sites (**Figure 14**). The modelling of site amplification effects in ground-motion prediction equations is

generally crude, using simple site classification schemes based on the average shear-wave velocity of the upper 30 m at the site and assuming that the degree of amplification is independent of the amplitude of the input motion, whereas it is generally observed that weak motion is amplified more than strong motion. For this reason, for site-specific predictions it is often preferred to predict the bedrock motions first and then model the dynamic response of the site separately (**Figure 15**).

The nature of ground shaking at a particular site during an earthquake is influenced by many factors, including the distribution and velocity of the slip on the fault rupture, the depth at which the fault rupture is located, the orientation of the fault rupture with respect to the travel path to the site, and the geological structure along the travel path and for several kilometres below the site. A situation that produces particularly destructive motions is the propagation of the fault rupture towards the site, which produces large-amplitude, high-energy pulses of velocity (**Figure 16**). The variable most often included in predictive equations after magnitude, distance and site classification is the style-of-faulting; equations that include the rupture mechanism as an explanatory variable all predict higher amplitudes of motion from reverse faulting earthquakes than from strike-slip events. The addition of this fourth explanatory variable, however, has an almost negligible impact on the scatter in the equations, with no appreciable reduction of the standard deviation.

Dense networks of accelerographs now exist in many countries around the world, but for many decades these were limited to a few regions such as California, Japan, Italy, Greece and Yugoslavia. In other regions, the number of available accelerograms is further reduced by the relatively low frequency of felt earthquakes. Seismic hazard assessment in such regions is hampered by the absence of indigenous recordings and a tool that is often employed is to use stochastic simulations to generate motions based on representing the ground shaking as random motion whose frequency content and duration are controlled by theoretical and empirical descriptions of seismic radiation and propagation (**Figure 17**).

Complete acceleration time-histories can also be generated using more sophisticated seismological models that model the source as a finite fault rupture. These simulations usually take the form of a kinematic model of the fault rupture, with rupture velocities and slip amplitudes specified across the fault plane (although these can be specified using statistical distribution in order to be able to generate a suite of motions for a given rupture). Dynamic fault-modelling, in which the stress conditions are specified and subsequent rupture is controlled by friction laws on the fault surface as well as the heterogeneous three-dimensional stress distribution, is less commonly used for the simulation of ground motions for engineering purposes because the necessary physical quantities are not known with sufficient precision and because the computational effort is much greater than with the kinematic models (which themselves can be quite demanding if lateral variations in geology are taken into account). In the future, as computers become more powerful and the details of the geologic structure and velocity

distributions are better determined, it is likely that the kinematic models will continue to be used, but the simulations will better represent the effects of wave propagation.

SEISMIC HAZARD ASSESSMENT

Engineering Seismology is often described as the link between the Earth sciences and engineering, and this is most evident in seismic hazard assessment, the aim of which is to estimate the earthquake ground-motions that can be expected at a particular location. Seismic hazard assessments may be performed for a number of reasons, the most common being to determine seismic loads to be considered in earthquake-resistant design of buildings. Another common application is the evaluation of the ground motions required as input to the assessment of landslide or liquefaction hazard. A rapidly expanding market for seismic hazard assessments is being created by the demand for earthquake loss models for local governments, emergency services, seismic code developers, and particularly the insurance and reinsurance industries.

There are many different ways to approach seismic hazard assessment, but all methods and approaches include two essential elements: a model for earthquake occurrence and a model for predicting ground motions from each earthquake. The starting point for building a model for earthquake occurrence, known as a seismicity model, is to first identify the locations where earthquakes will be expected to occur in the future. Data used to define seismic source zones include previous earthquake activity, the existence of geological faults, and crustal deformations. Ideally, all seismic sources should be identified as active geological faults, but this is very often not possible, whence zones are defined as areas within which future earthquakes are expected to occur (**Figure 18**). Some recent approaches to seismic hazard assessment dispense with source zones altogether, basing the sources of postulated future events on past activity. The catalogue of instrumentally-recorded earthquakes extends back at very most to 1898, which is a very short period of observation for events whose recurrence intervals can extend to hundreds or even thousands of years. For this reason, great value is to be obtained from extending the catalogue through the careful interpretation of historical records, making use of empirical relationships between magnitude and intensity referred to previously.

Although the distinction masks many equally marked differences amongst the various methods that fall within each camp, a basic division exists between deterministic and probabilistic approaches to seismic hazard assessment. In the deterministic approach, only a few earthquake scenarios are considered, and sometimes just one, selected to represent an approximation to the worst case. The controlling earthquake will generally correspond to an event with the nominal maximum credible magnitude, located at the closest location to the site within the seismogenic source; the ground motion is generally calculated as the 50- or 84-percentile value from the prediction equation. In the probabilistic approach, all possible earthquake scenarios are considered, including events of every magnitude from the minimum considered to be of engineering significance (~ 4) up to the maximum credible, occurring at every possible location with

the source zones, and for each magnitude-distance combination various percentiles of the motion are considered to reflect the scatter in the ground-motion prediction equations. Alternative options for the input parameters may be considered by using a logic-tree formulation, in which weights are assigned to different options that reflect the relative confidence in their being the best representation (**Figure 19**). The output is a ranking of these earthquake scenarios in terms of the ground-motion amplitudes that they generate at the site and their frequency of occurrence (**Figure 20**).

Seismic hazard assessment can be carried out for an individual site, the output including a response spectrum calculated ordinate by ordinate, or even a suite of accelerograms. Hazard assessment is often performed for regions or countries, deriving hazard curves for a large number of locations and then drawing contours of a ground-motion parameter (most often PGA) for a given annual frequency of occurrence, which is often expressed in terms of its inverse known as a return period (**Figure 21**). Such hazard maps in terms of PGA are the basis of zonation maps included in seismic design codes, from which design response spectra are constructed by anchoring a spectral shape selected for the appropriate site class to the PGA value read from the zonation map.

ACKNOWLEDGEMENTS

We thank John Douglas, Gabriel Toro, José Luis de Justo Alpañés, Paul Somerville and Iain Tromans for providing data and figures, and Juliet Bird and Fleur Strasser for their helpful comments on a draft of the manuscript.

See Also

Engineering Geological Aspects of Earthquakes, Earthquake (Earth Processes), Faults, Geohazards: Natural, Liquefaction, Slumps and Slides, Tsunamis.

Further Reading

Abrahamson, NA (2000) State of the practice of seismic hazard evaluation. *GeoEng 2000*, Melbourne, Australia, 19-24 November.

Ambraseys NN (1988) Engineering seismology. *Earthquake Engineering & Structural Dynamics* 17: 1-105.

Beskos DE and Anagnostopoulos SA (1997) *Computer Analysis and Design of Earthquake Resistant Structures: A Handbook*. Computational Mechanics Publications (Chapters 3-5).

Bommer JJ (2003) Uncertainty about the uncertainty in seismic hazard analysis. *Engineering Geology* 70: 165-168.

Boore DM (1977) The motion of the ground in earthquakes. *Scientific American* 237: 68-78.

Boore DM (2003) Simulation of ground motion using the stochastic method. *Pure and Applied Geophysics* 160: 635-676.

Chen W-F and Scawthorn C (2003) *Earthquake Engineering Handbook*. CRC Press, Boca Raton, FL. (Chapter 1-10).

Douglas J (2003) Earthquake ground motion estimation using strong-motion records: a review of equations for the estimation of peak ground acceleration and response spectral ordinates. *Earth Science Reviews* 61: 43-104.

Giardini D and Basham P (1993) Technical planning volume of the ILP's global seismic hazard assessment program for the UN/IDNDR. *Annali di Geofisica* 36(3/4): 3-257.

Giardini D (1999) The global seismic hazard assessment program (GSHAP) 1992-1999: summary volume. *Annali di Geofisica* 42: 957-1230.

Hudson DL (1979) *Reading and Interpreting Strong Motion Accelerograms*. EERI Monograph, Earthquake Engineering Research Institute, Oakland, California.

Jackson JA (2001) Living with earthquakes: know your faults. *Journal of Earthquake Engineering* 5(special issue 1): 5-123.

Kramer SL (1996) *Geotechnical Earthquake Engineering*. Prentice-Hall.

Lee WHK, Kanamori H, Jennings PC and Kisslinger C (2003) International Handbook of Earthquake and Engineering Seismology, Part B. Academic Press. (Chapters 57-64).

McGuire RK (2003) *Seismic Hazard and Risk Analysis*. EERI Monograph MNO-10, Earthquake Engineering Research Institute, Oakland, California.

Naeim F (2001) *The Seismic Design Handbook*, 2nd Edition. Kluwer Academic Publishers. (Chapters 1-3).

Reiter L (1990) *Earthquake Hazard Analysis: Issues and Insights*. Columbia University Press.

Table 1. Summary of the 1998 European Macroseismic Intensity scale in terms of observed effects on people and buildings.

Intensity	Definition	Effects on People and Buildings
I	Not felt	Not felt – only detected by sensitive instruments
II	Scarcely felt	Felt by very few people, who are in particularly favourable conditions at rest and indoors
III	Weak	Felt by a few people, mostly those at rest
IV	Largely observed	Felt by many people indoors and very few outdoors; a few people are woken by the shaking
V	Strong	Felt by most people indoors and a few outdoors; a few people are frightened and many who are sleeping are woken by the shaking
		Fine cracks in a few of the most vulnerable types of buildings, such as adobe and unreinforced masonry
VI	Slightly damaging	Shaking felt by nearly everyone indoors and by many outdoors; a few people lose their balance
		Minor cracks in many vulnerable buildings, and a few poor quality reinforced concrete (RC) structures; a few of the most vulnerable buildings have cracks in walls and spalling of fairly large pieces of plaster
VII	Damaging	Most people are frightened by the shaking, and many have difficult standing, especially those on upper stories of buildings
		Many adobe and unreinforced masonry buildings sustain large cracks and damage to roofs and chimneys; some will have serious failures in walls and partial collapse of roofs and floors; minor cracks in RC structures with some earthquake-resistant design, more significant cracks in poor quality RC structures
VIII	Heavily damaged	Many find it difficult to stand.
		Many vulnerable buildings experience partial collapse and some collapse completely; large and extensive cracks in poor quality RC buildings, and many cracks in RC buildings with some degree of earthquake-resistant design
IX	Destructive	General panic (this is the highest degree of intensity that can be measured from human response)
		General and extensive damage in vulnerable buildings; cracks in columns, beams and partition walls of RC buildings, some of those of poor quality suffering heavy structural damage and partial collapse; non-structural damage in RC structures with high level of earthquake-resistant design
X	Very destructive	Partial or total collapse in nearly all vulnerable buildings; extensive structural damage in RC and steel structures.
XI	Devastating	Extensive damage and widespread collapse in nearly all building types; very rarely observed, if ever.
XII	Completely devastating	Cataclysmic damage; has never been observed and is probably not physically realisable

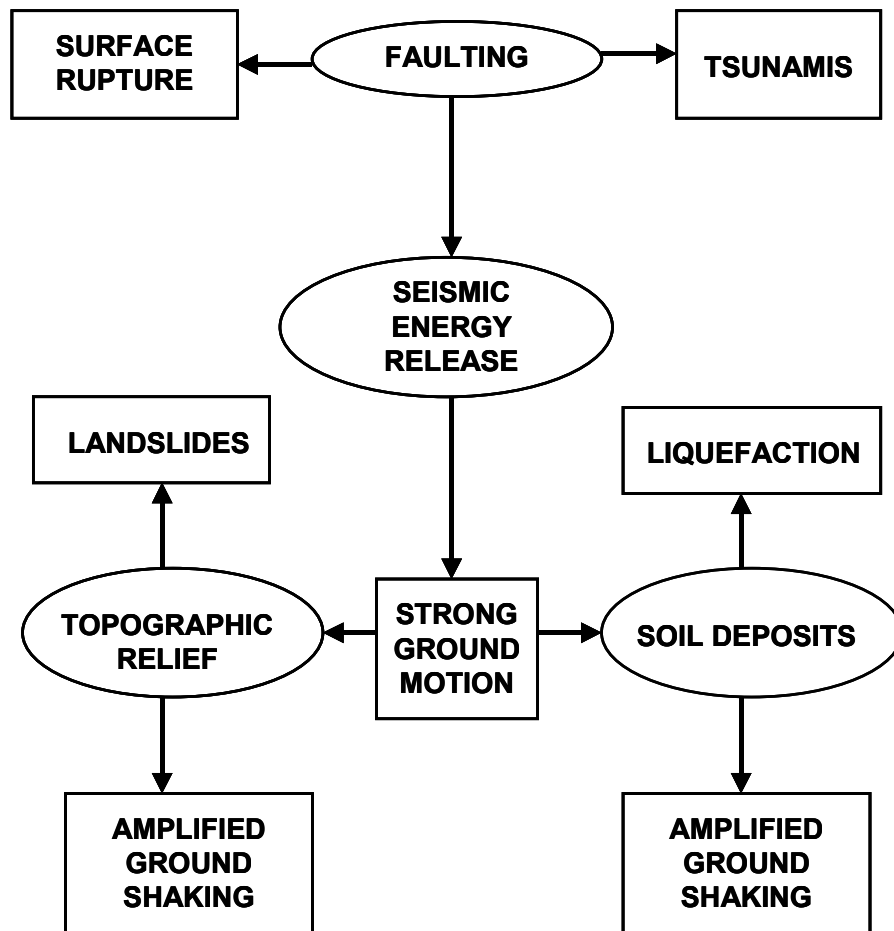


FIGURE 1. Potentially destructive effects of earthquakes. The ovals are elements of the earthquake generation process and the natural environment; the rectangles are the resulting seismic hazards.

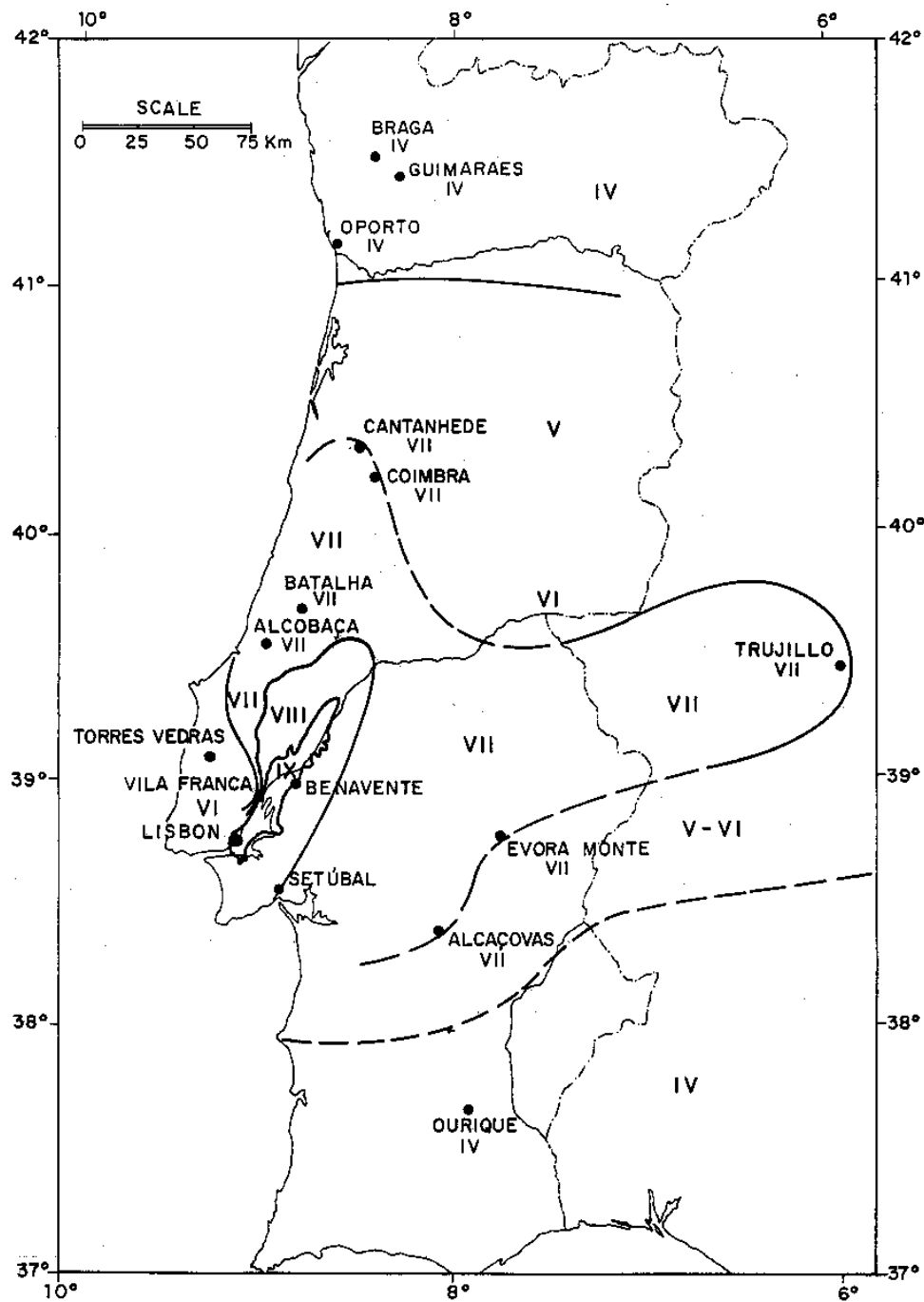


FIGURE 2a. Regional isoseismal map of the Lisbon earthquake of January 1531.

[From: J.L. Justo & C. Salwa (1998) The 1531 Lisbon earthquake. *Bulletin of the Seismological Society of America* **88**(2), 319-328. Permission requested from SSA].

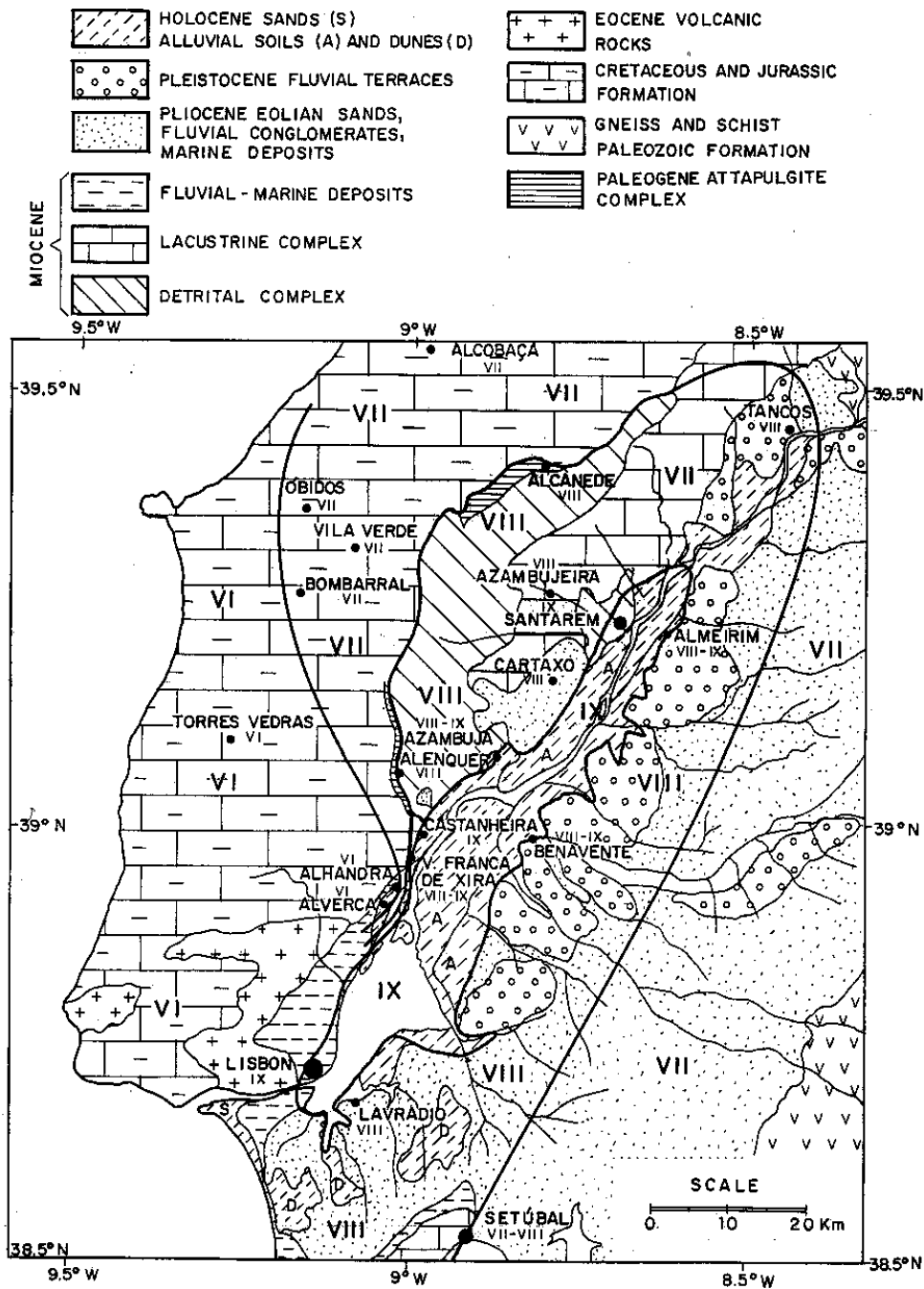


FIGURE 2b. Isoseismal map for the epicentral area of the Lisbon earthquake of January 1531, superimposed on a map of the local geology.

[From: J.L Justo & C. Salwa (1998) The 1531 Lisbon earthquake. *Bulletin of the Seismological Society of America* 88(2), 319-328. *Permission requested from SSA*].

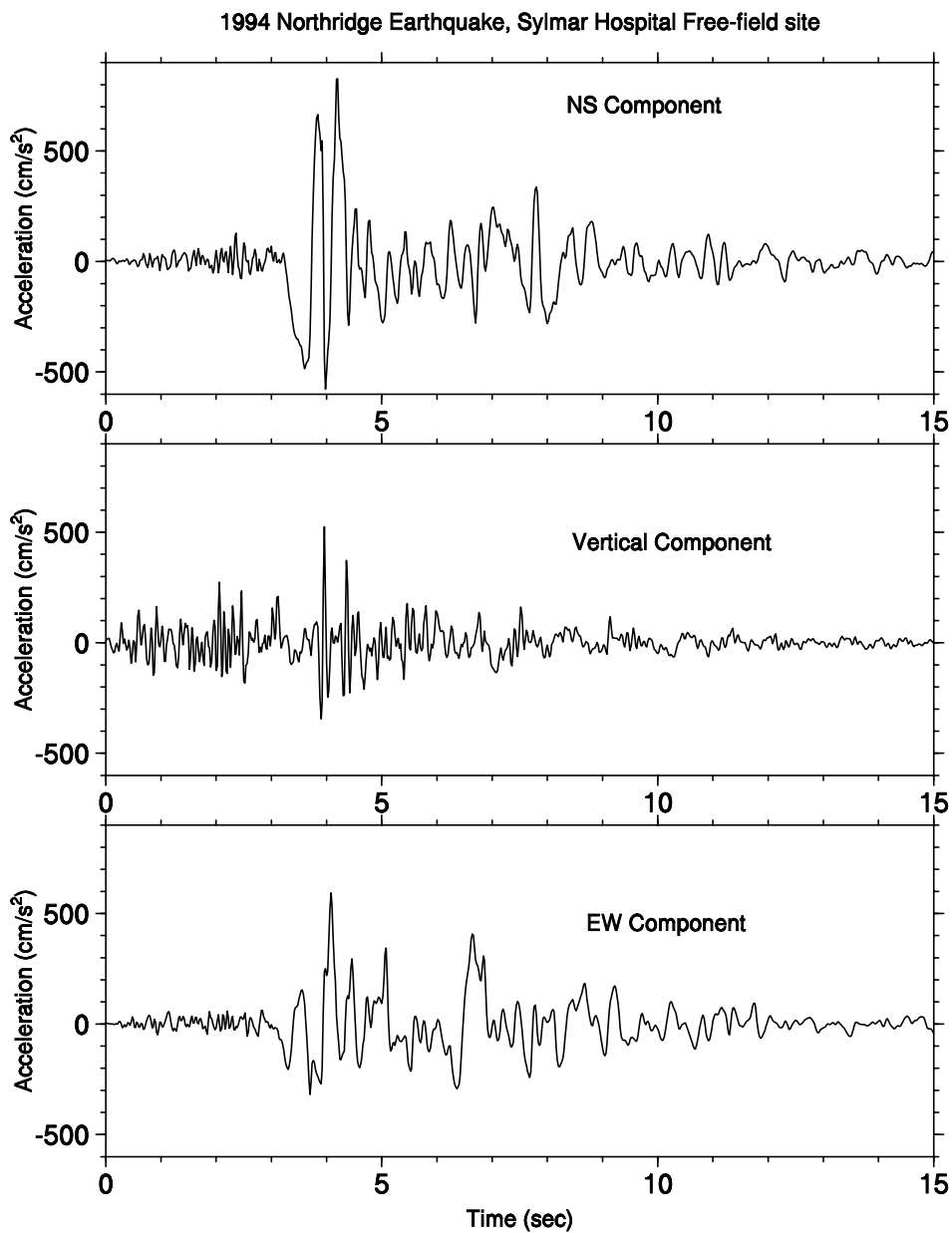


FIGURE 3. Three-component accelerogram recorded at Sylmar Hospital during the Northridge, California, earthquake of January 1994.

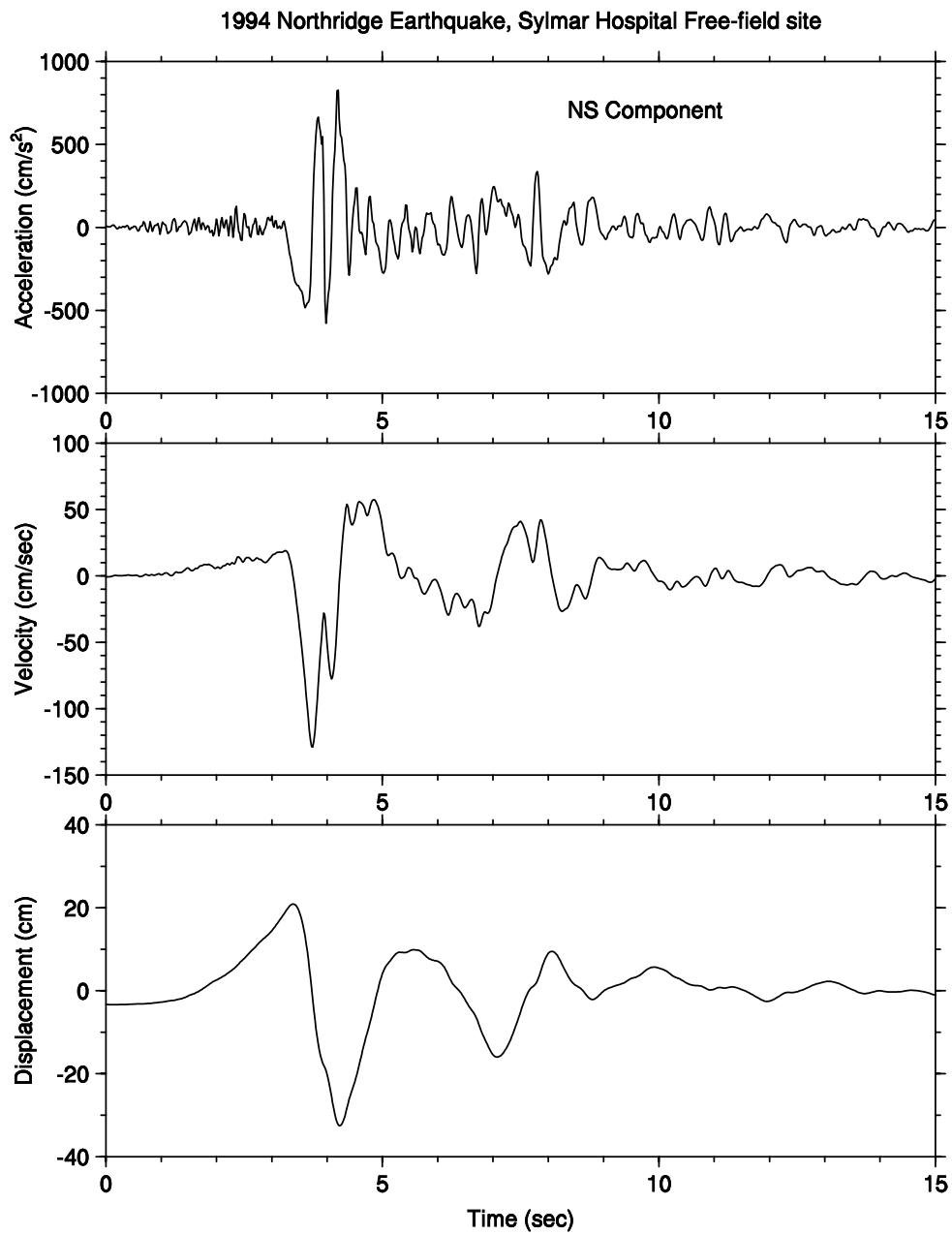


Figure 4. Acceleration, velocity and displacement time-series from the north-south horizontal component of the Sylmar record.

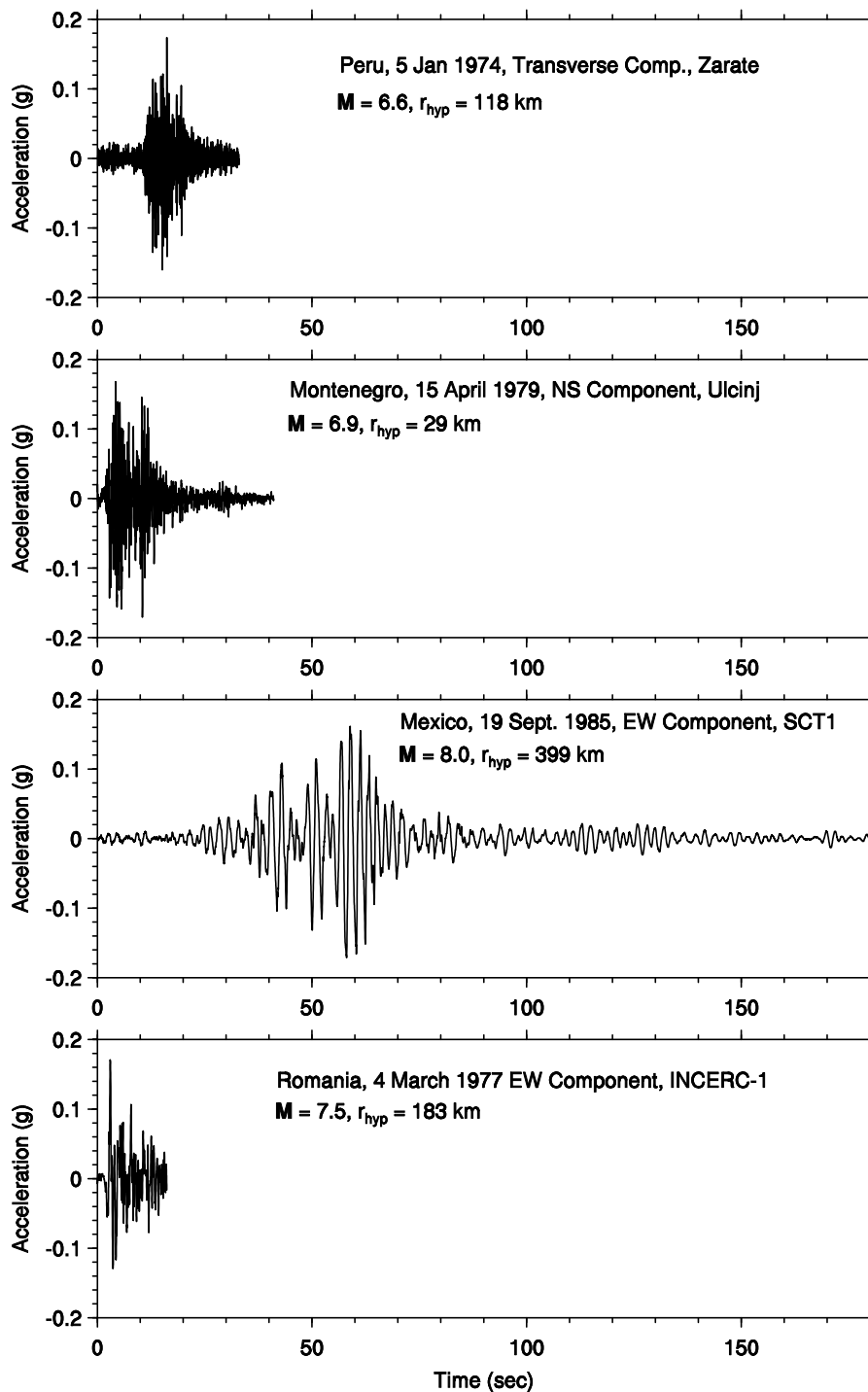


Figure 5. Four horizontal accelerogram components with exactly the same PGA

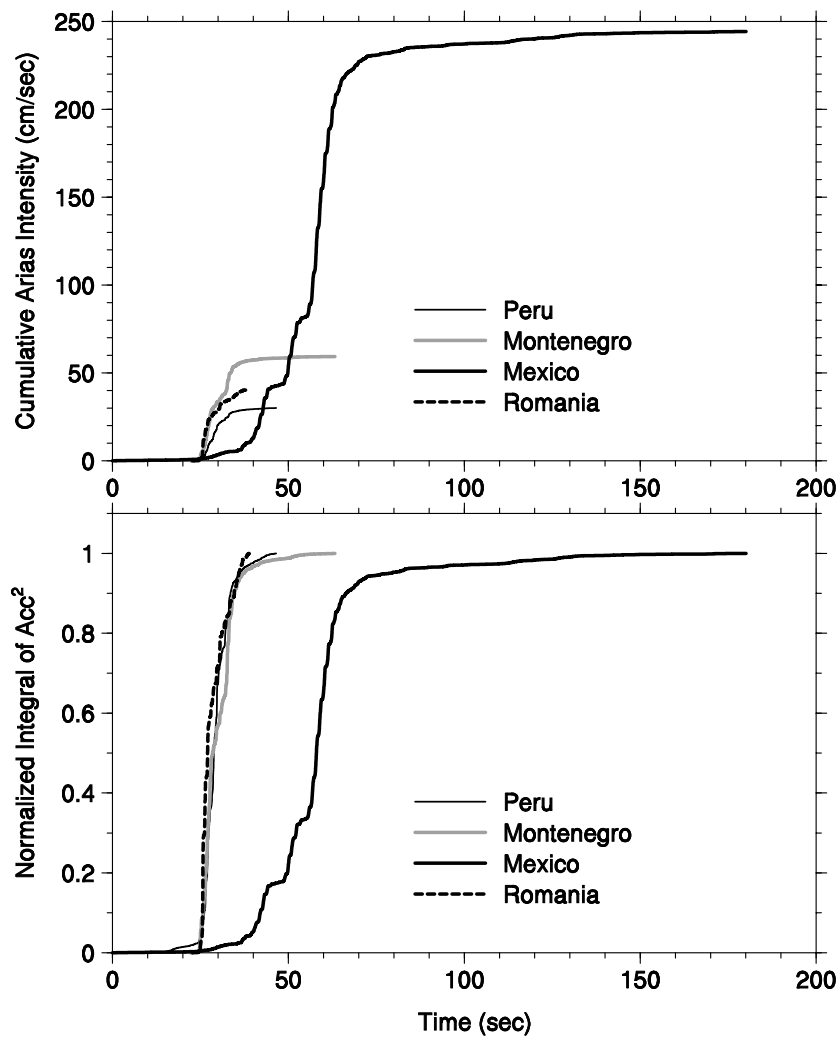


Figure 6. Husid plots for the four acceleration time-series shown in Fig. 5, showing the build-up of Arias intensity with time. The upper plot shows the absolute values of Arias intensity; in the lower plot the curves are normalised to the maximum value attained.

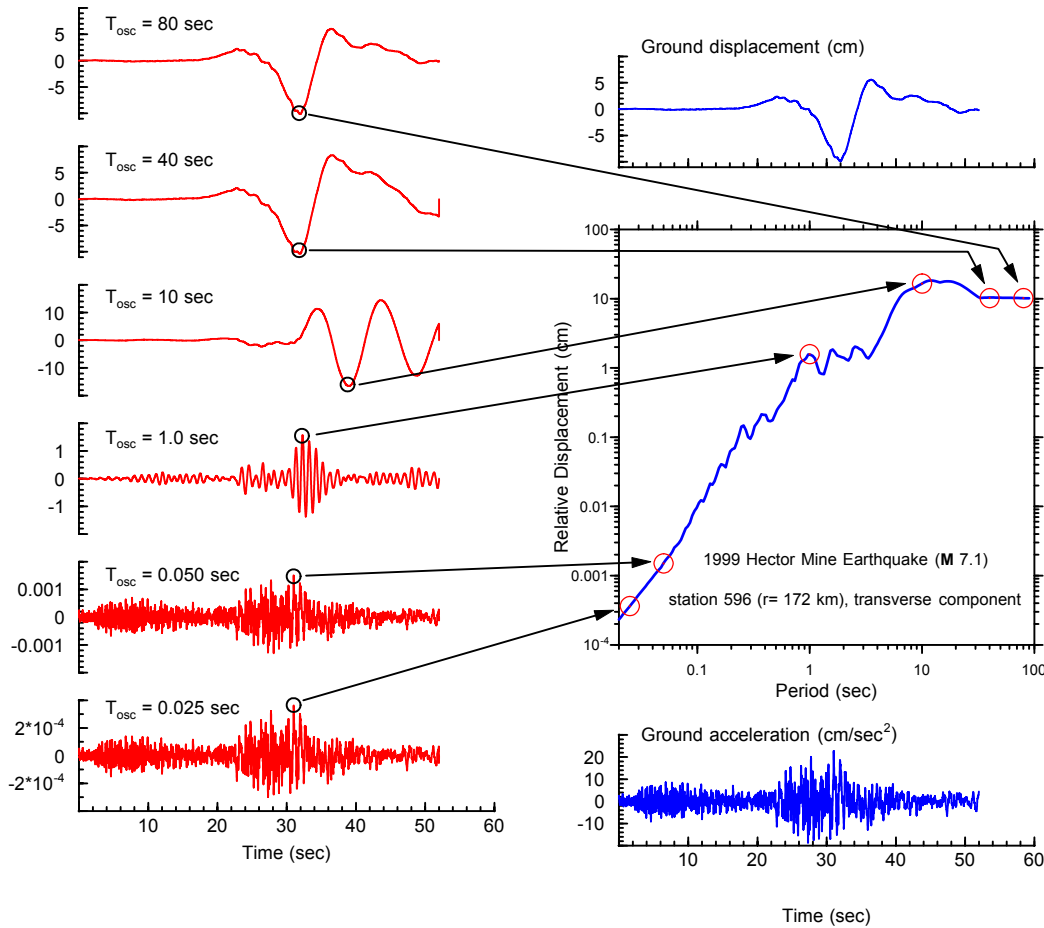


Figure 7. Illustration of the concept of the response spectrum. The trace in the lower right-hand corner is the ground acceleration, and the traces on the left-hand side of the figure are the displacement response time-series for simple oscillators with different natural periods of vibration. The maximum displacement of each oscillator is plotted against its natural period to construct the response spectrum of relative displacement. The lowest two traces in the figure illustrate that for short-period oscillators, the response mimics the ground acceleration; whereas for long-period oscillators the response imitates the ground displacement, shown in the upper right-hand corner.

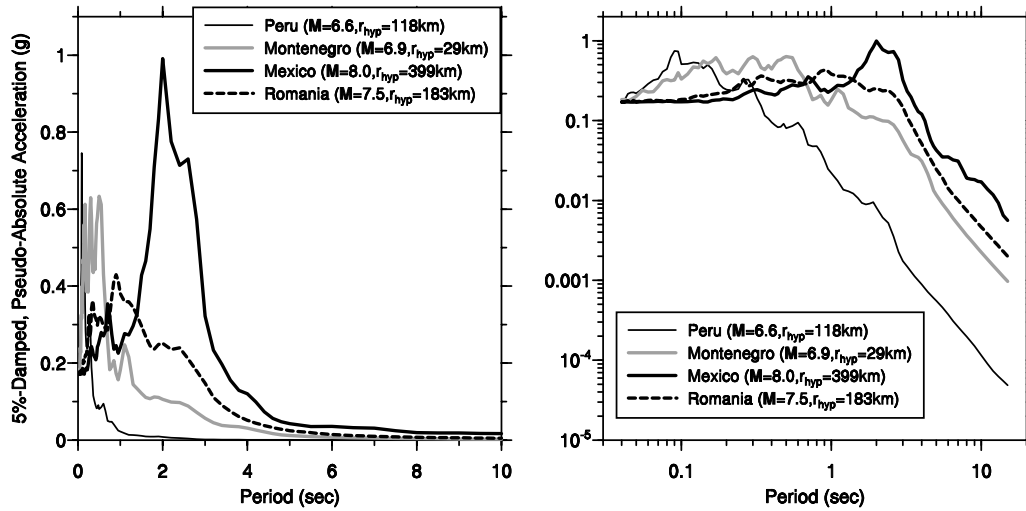


Figure 8 Acceleration response spectra (5% damped) of the four accelerograms shown in Figure 5; the plots are identical except that the one on the left uses linear axes, the one on the right logarithmic axes. Each type of presentation is useful for viewing particular aspects of the motion, depending on whether the interest is primarily at short or long periods of response.

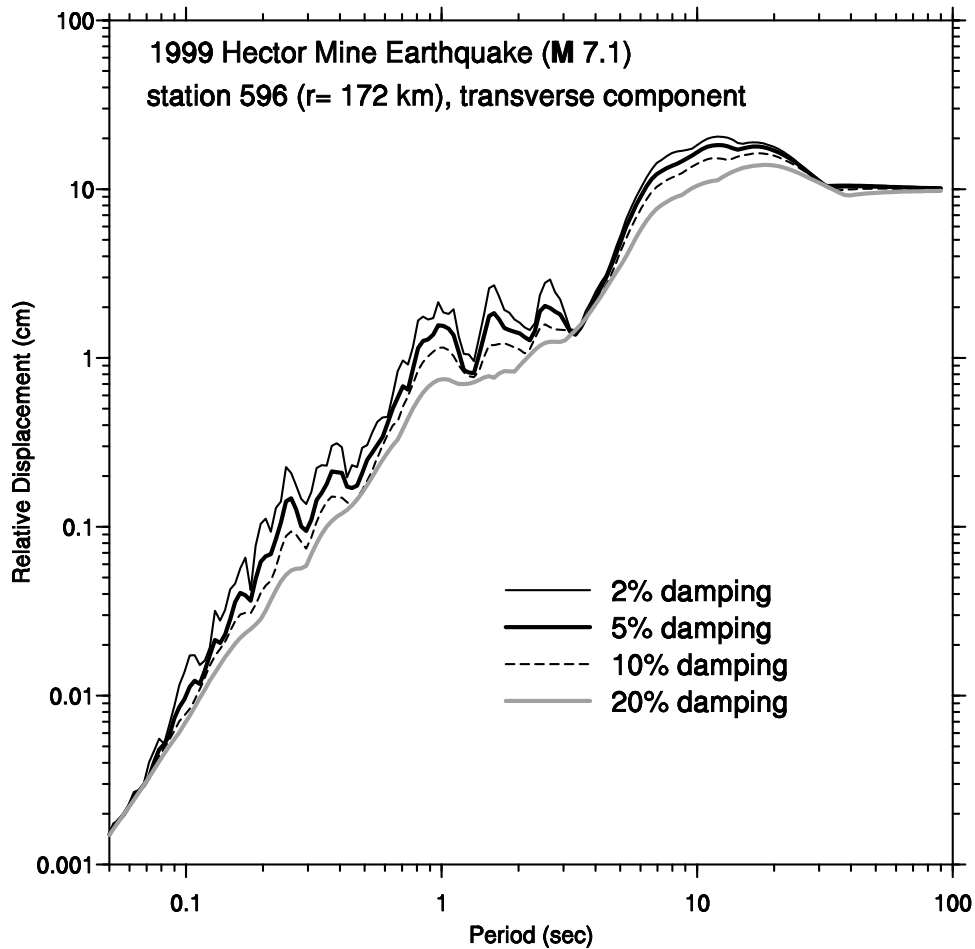


Figure 9. Displacement response spectra of a single accelerogram from the 1999 Hector Mine earthquake in California, plotted for different levels of damping. The spectra all converge to the values of peak ground acceleration and displacement at very short and very long periods, respectively.

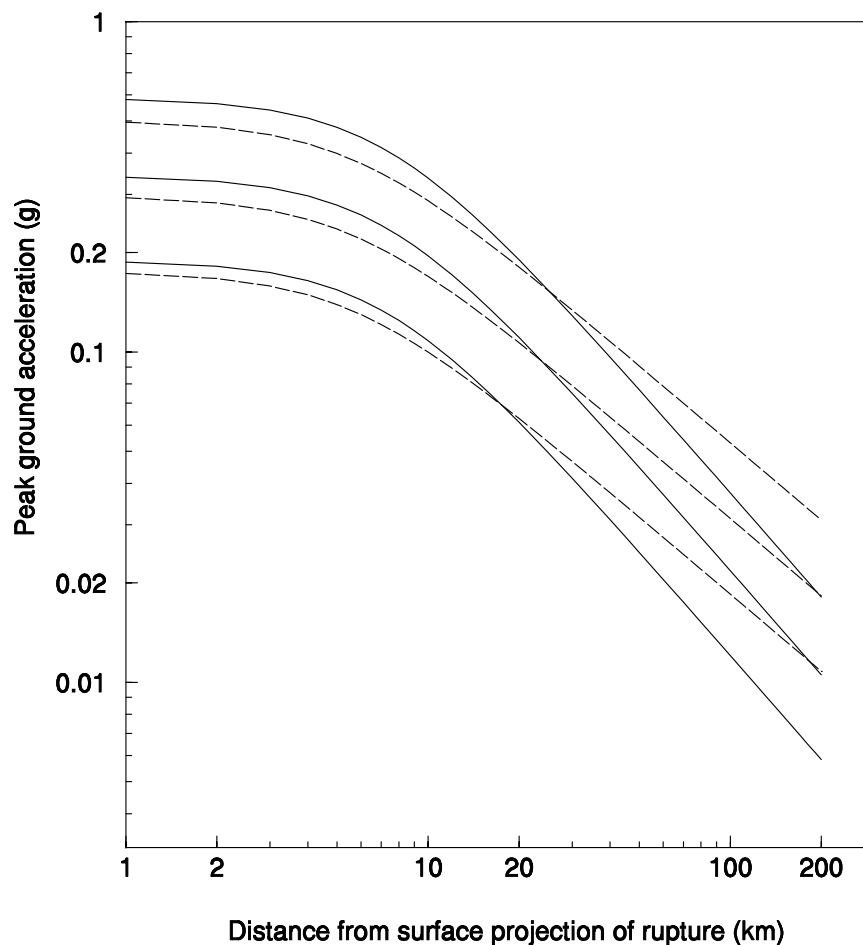


FIGURE 10.

Predicted median values of PGA as a function of distance for earthquakes of moment magnitude 5.5, 6.5 and 7.5, using equations derived from western North American (solid lines) and European (dashed lines) data sets. The European equation is based on surface-wave magnitude, so an appropriate empirical conversion has been used. The equations are based on different definitions of the horizontal component, the European equation using the larger of the two horizontal accelerations, the North American equation using their geometric mean; the former definition, on average, yields values about 1.17 times larger than the latter. Different criteria were used in the two studies for selecting records, especially at greater distances, for regression. In light of these various observations, it is not possible to draw conclusions about differences or similarities in strong ground-motions between the two regions. The North American equation is from Boore, Joyner & Fumal, *Seismological Research Letters* (1997), vol. 68, no. 1, pp. 128-153; the European equation is from Tromans & Bommer, *Proceeding of the 12th European Conference on Earthquake Engineering* (2002), London, Paper no. 394.

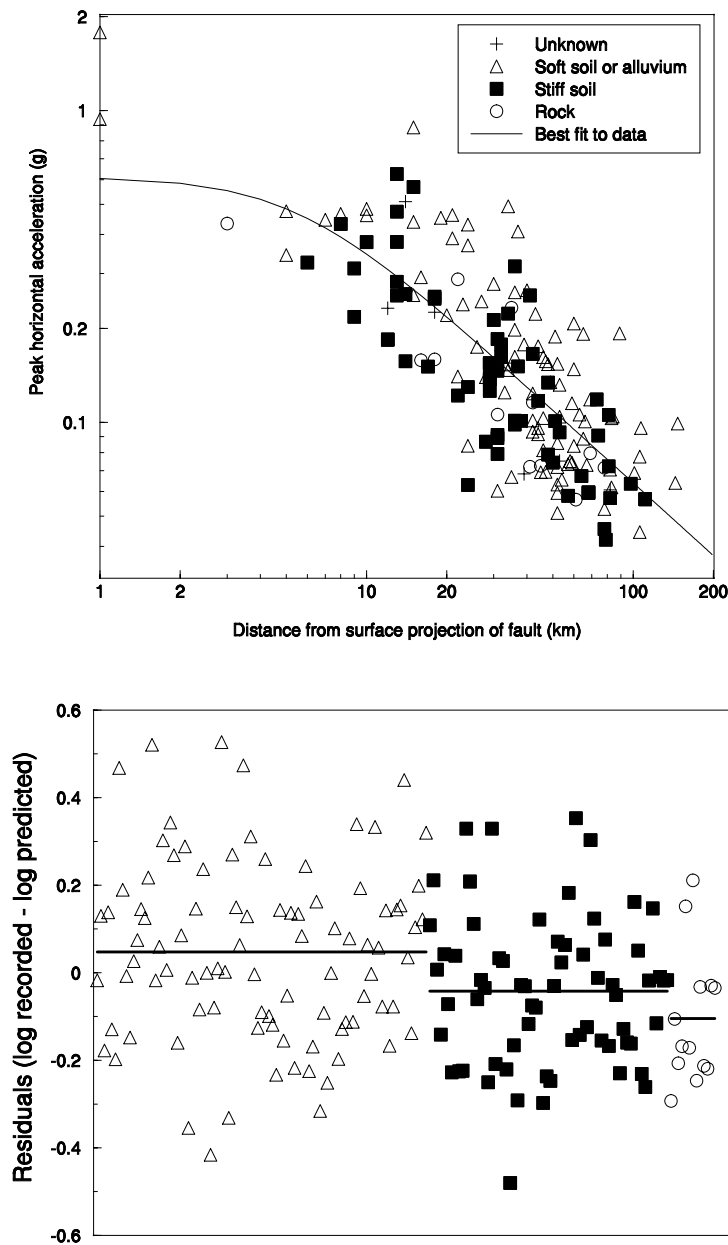


Figure 11. *Upper:* Values of peak horizontal ground acceleration recorded in the 1994 Northridge earthquake in California, plotted as a function of distance from the earthquake source with an indication of the surface geology at the recording site. The solid line is the result of a regression on the data using a typical model employed in ground motion prediction equations. *Lower:* Residuals group by site class; the horizontal lines show the mean of the residuals in each class, which show that there is a tendency for stronger motions on softer ground. However, the differences between the mean lines is small compared with the overall dispersion, whence inclusion of site classification in the predictive equation would result in only a modest reduction of the aleatory variability.

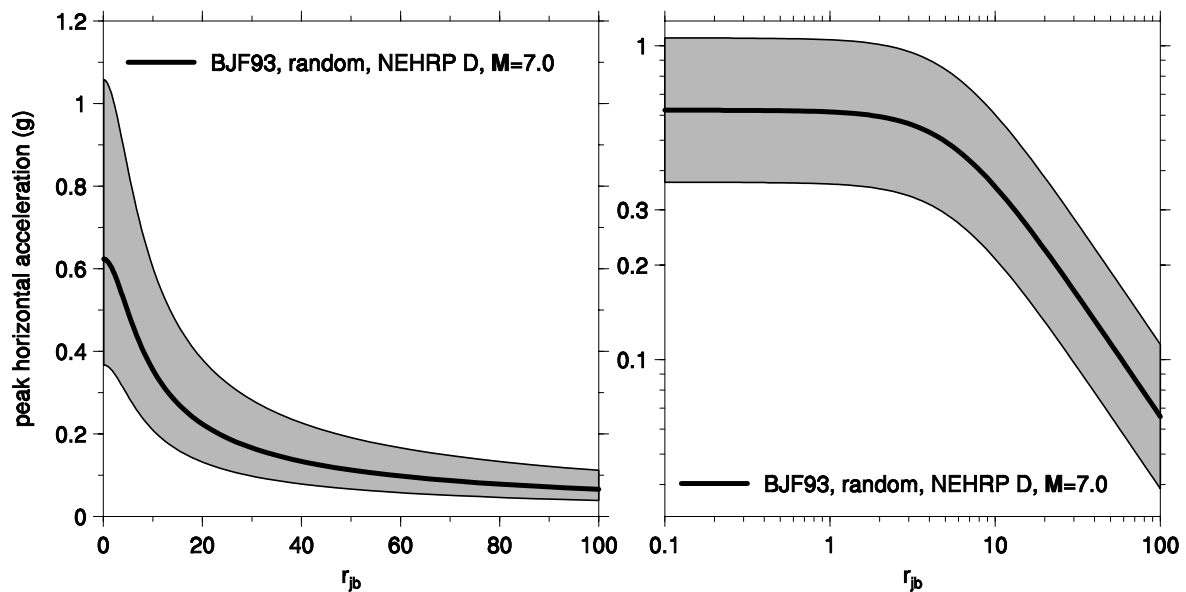


Figure 12. Predicted values of horizontal PGA on soft soil (class D) sites for an earthquake of magnitude 7 as a function of distance from the surface projection of the fault rupture. The predictions are made using an equation derived from earthquakes recorded in western North America, by Boore, Joyner & Fumal, *US Geological Survey Open-File Report 93-509* (1993). The thick black line shows the median predicted values, the grey bands indicate the range of the median multiplied and divided by 10^0 ; on average, 68% of observations would be expected to fall within the grey area.

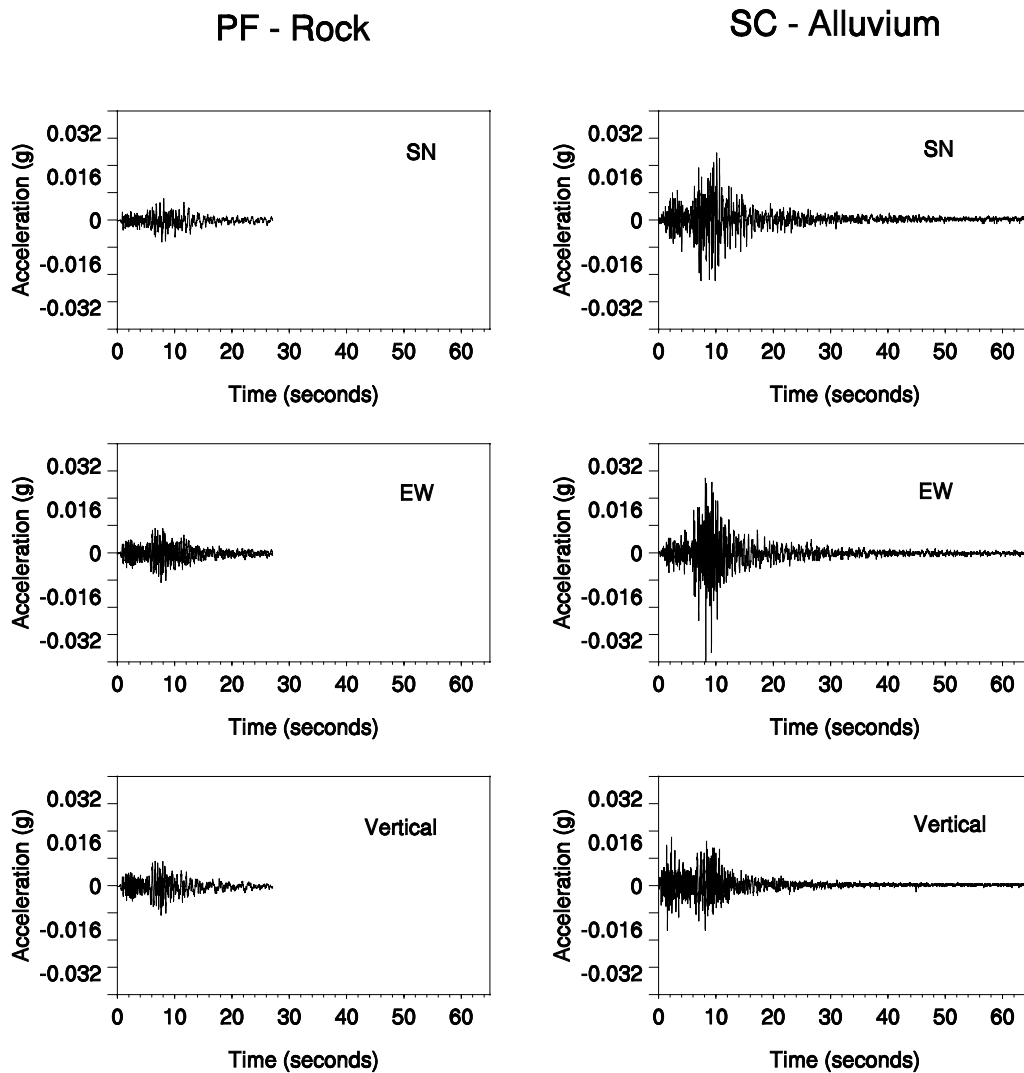


Figure 13. Accelerograms recorded on two instruments in the Gemona (Italy) array during the M_w 5.6 Bovak (Slovenia) earthquake of 12 April 1998. Both instruments are 38 km from the earthquake epicentre, and separated by about 700 m. The station PF (Piazza del Ferro) is on bedrock with a shear-wave velocity reported as 2,500 m/s, whereas station SC (Scugelars) is on alluvium with a shear-wave velocity of 500 m/s. Since the distance and azimuth of the two stations with respect to the earthquake source are almost identical, the difference between the amplitude of the two recordings is primarily due to the different surface geology at the two recording locations.

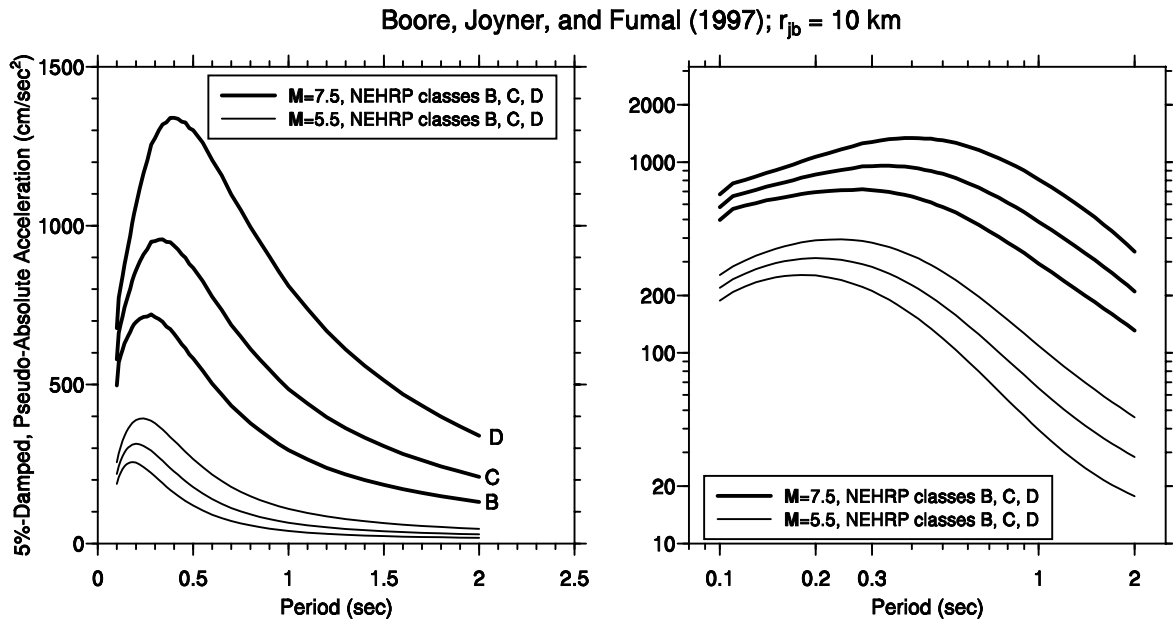


Figure 14. Predicted median ordinates of spectral acceleration (5% damped) for a magnitude 5.5 (thin lines) and a magnitude 7.5 (thick lines) earthquake recorded at 10 km on sites classified as B, C and D in the NEHRP scheme, corresponding to soft rock, stiff soil and soft soil respectively. The two graphs are identical except for the left-hand plot being on linear axes, the right-hand plot on logarithmic axes.

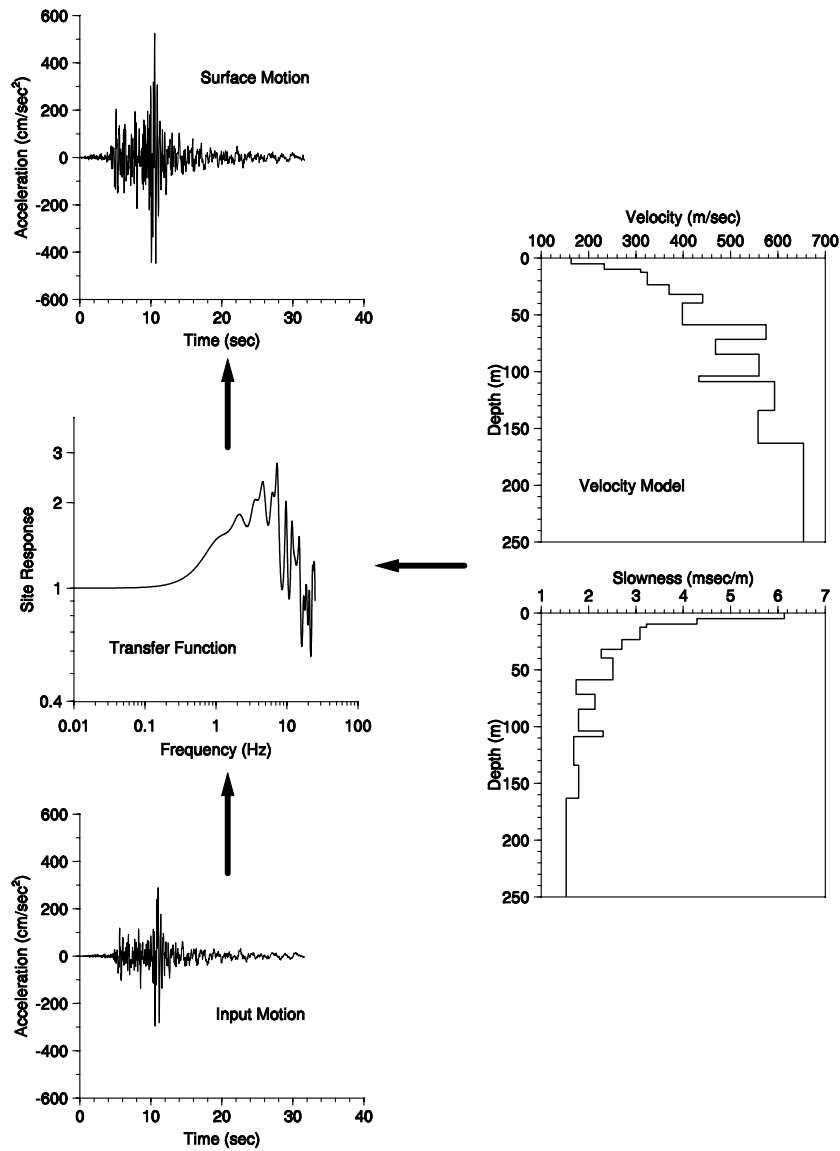


Figure 15. Illustration of site response analysis: The input motion in the underlying rock (*bottom left*) passes through a model of soil profile to produce the surface motions (*top left*). The soil characteristics are represented by both the shear-wave velocity and the shear-wave slowness profiles (*right*); the slowness is simply the reciprocal of the shear-wave velocity, but there are many reasons for using it in place of the velocity. The theoretical response of layered systems involves travel times across the layers, which are directly proportional to the slowness; the proportionality to velocity is inverse. Furthermore, to obtain a representative profile for a soil class using several boreholes, individual measures slowness can be directly averaged, whereas it is not correct to do this for velocities. Finally, the largest influence on the surface motion is due to the differences in velocities near the surface, and these differences become more clearly apparent when the slowness profile is shown; larger velocity differences in the stiffer layers at greater depths, which can dominate a velocity profile, are less important.

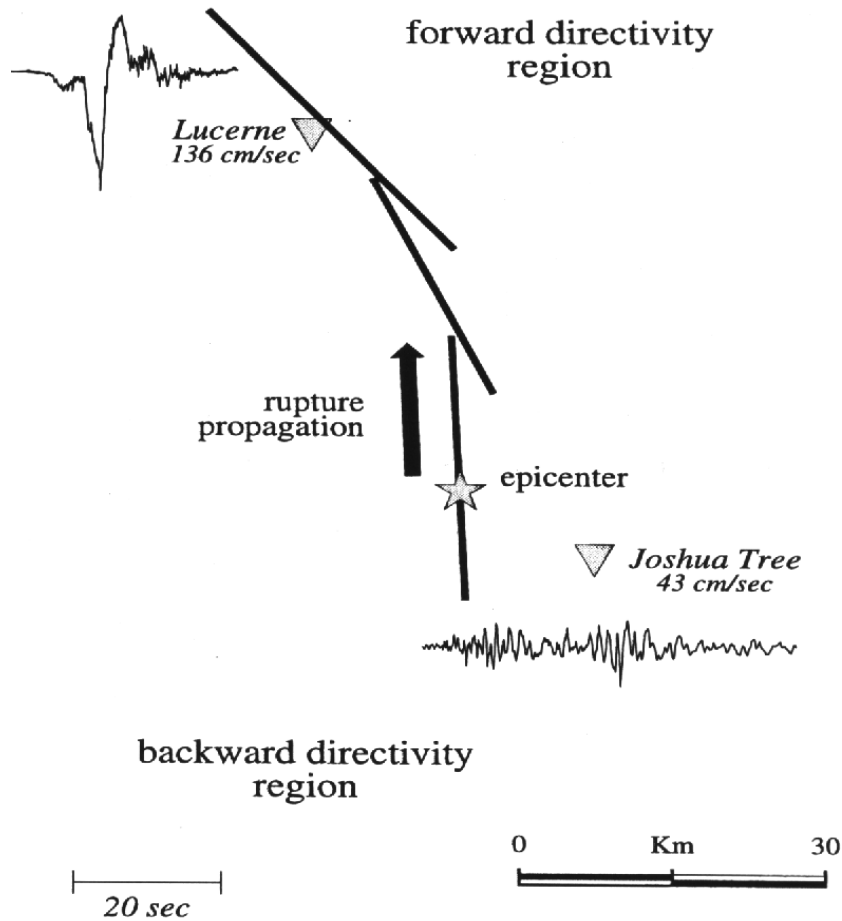


FIGURE 16.

Velocity time-series obtained from integration of horizontal accelerograms recorded at Lucerne and Joshua Tree stations during the 1992 Landers earthquake in California. The fault rupture propagated towards Lucerne and away from Joshua Tree, creating forward directivity effects (short duration shaking consisting of a concentrated high-energy pulse of motion) at the former, and backward directivity effects (long duration shaking of several small pulses of motion) at the latter.

[From: Somerville, PG, Smith, NF, Graves, RW and Abrahamson, NA (1997) Modification of empirical strong ground motion attenuation relations to include the amplitude and duration effects of rupture directivity. *Seismological Research Letters* 68(1), 199-222. Permission requested from SSA].

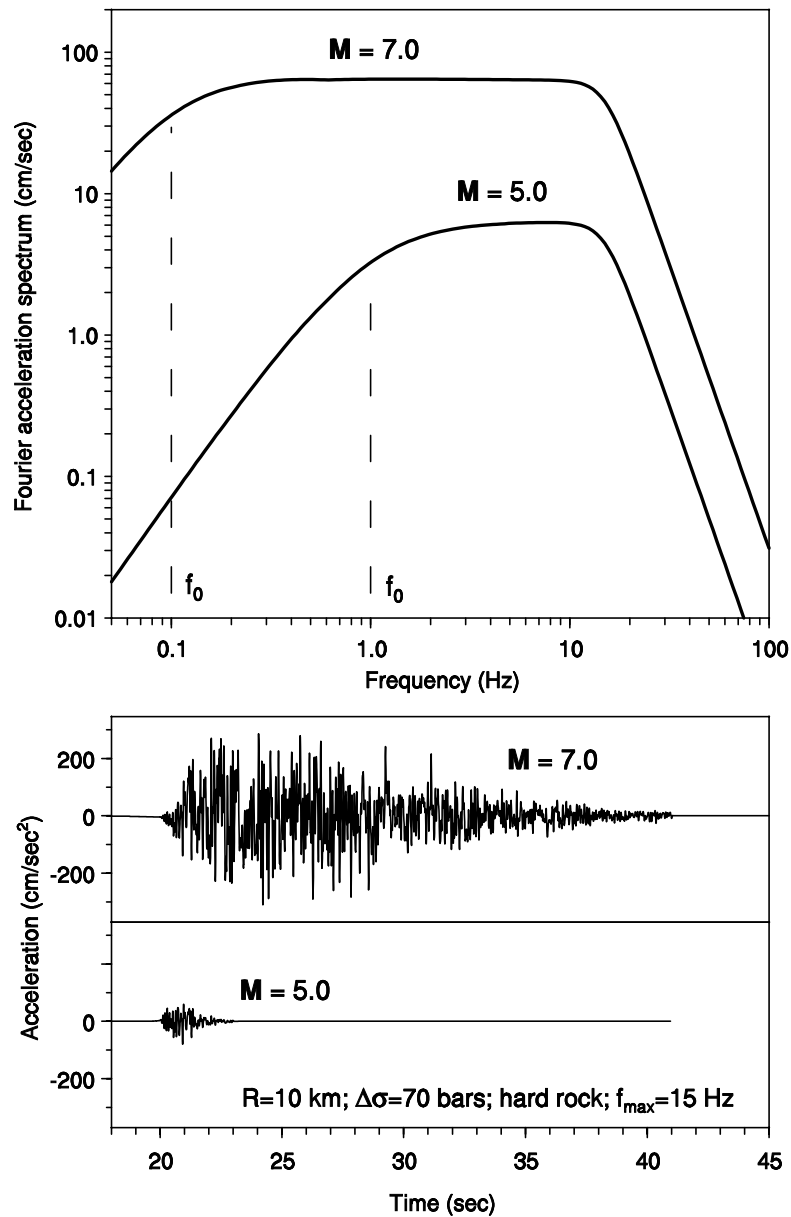


FIGURE 17.

Theoretical Fourier spectra for earthquakes of magnitude 5 and 7 at 10 km from a rock site, assuming a stress parameter of 70 bars. The lower part of the figure shows stochastic acceleration time-series generated from these spectra, from which the influence of magnitude on amplitude and duration (or number of cycles) can be clearly observed. From the spectra in the upper part of the figure it can be appreciated that scaling with magnitude is frequency-dependent, with larger magnitude events generating proportionally more long-period radiation.

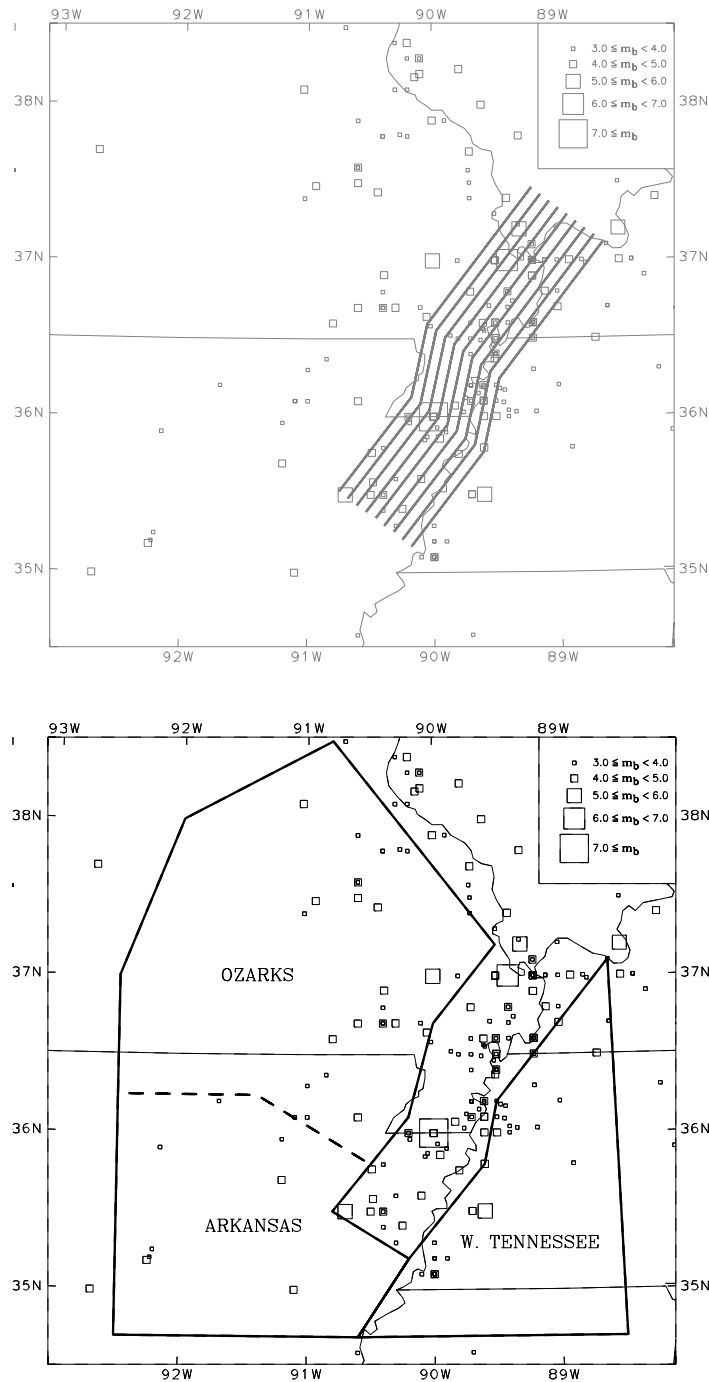


FIGURE 18. Seismic sources used for probabilistic hazard study of the Mississippi embayment. The upper figure shows the New Madrid seismic source zone represented as a number of parallel hypothetical faults; the lower figure shows the area sources used to represent seismicity not associated with the New Madrid zone.

[From: Toro, GR, Silva, WJ, McGuire, RK and Herrmann, RB (1992) Probabilistic seismic hazard assessment of the Mississippi Embayment. *Seismological Research Letters* **63**(3), 449-475. Permission requested from SSA].

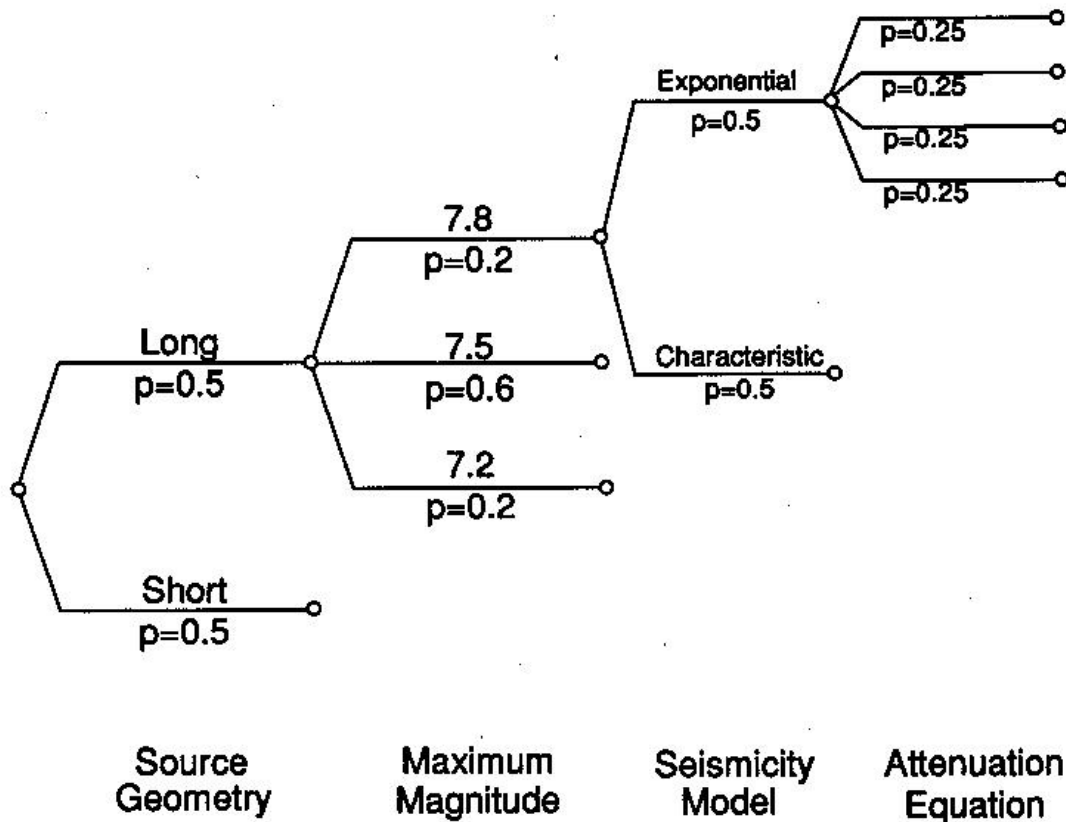


FIGURE 19.

Logic-tree formulation for probabilistic seismic hazard study of the Mississippi embayment. For different input parameters, different options are considered at each node, which are then assigned weights (p) to reflect the relative confidence in each option; the values of p at each node always sum to unity. The source geometry options are the faults shown in Fig. 18, and an alternative model in which the faults are longer.

[From: Toro, GR, Silva, WJ, McGuire, RK and Herrmann, RB (1992) Probabilistic seismic hazard assessment of the Mississippi Embayment. *Seismological Research Letters* **63**(3), 449-475. Permission requested from SSA].

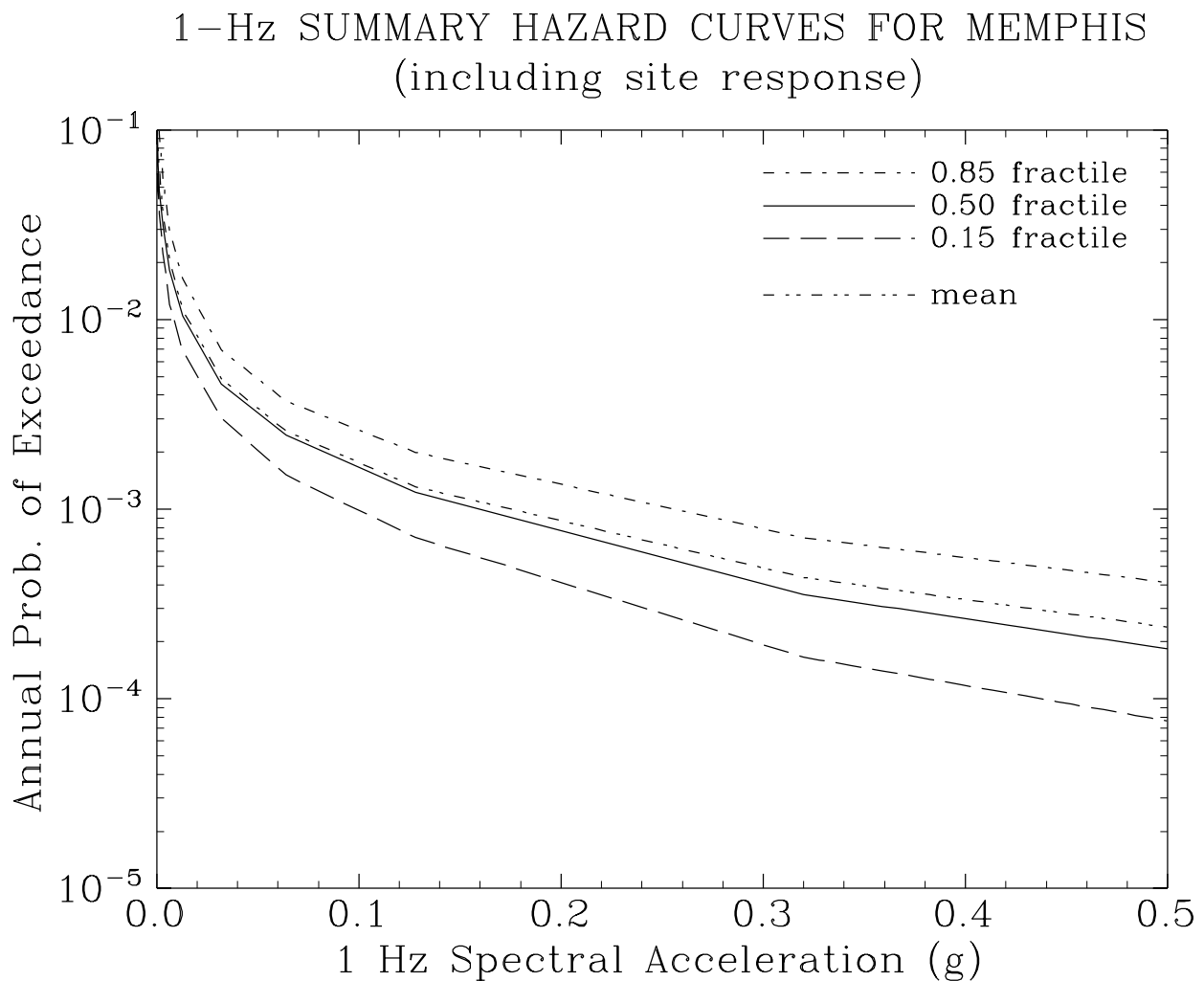


FIGURE 20. Seismic hazard curves for spectral acceleration at 1 second response period for Memphis, obtained using the logic-tree formulation in Fig. 19.

[From: Toro, GR, Silva, WJ, McGuire, RK and Herrmann, RB (1992) Probabilistic seismic hazard assessment of the Mississippi Embayment. *Seismological Research Letters* **63**(3), 449-475. Permission requested from SSA].

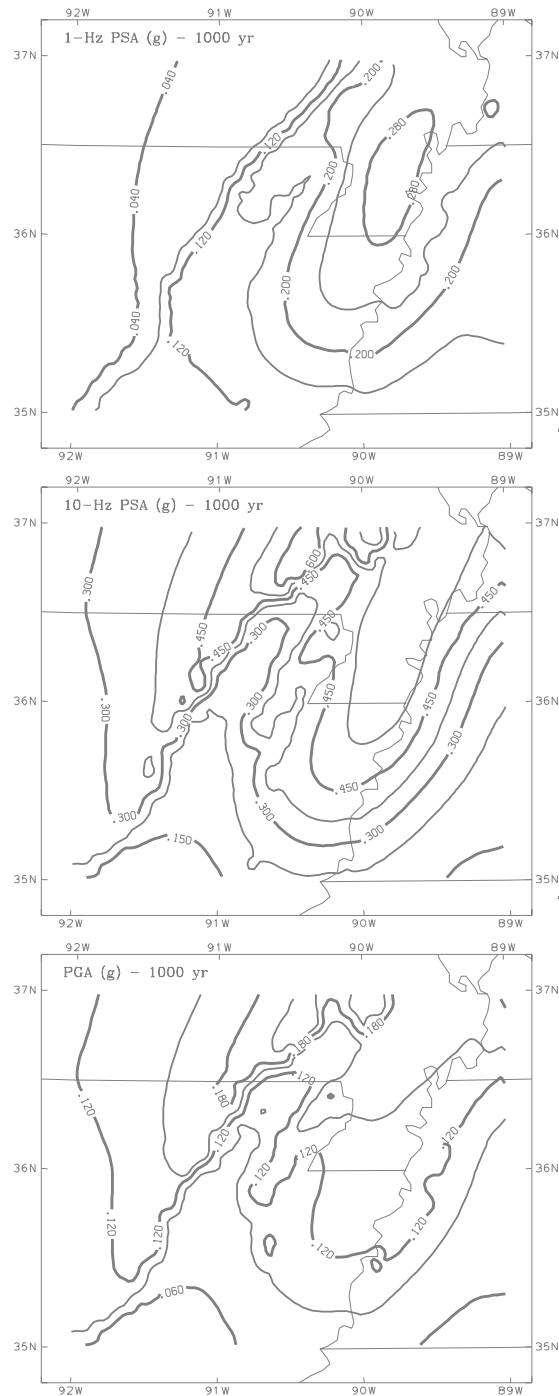


FIGURE 21. Contours of spectral accelerations in the Mississippi embayment with 1,000 year return period, for different response periods: (*from top to bottom*) 1.0 second, 0.1 second and PGA. The maps show the spectral accelerations read from the mean hazard curve.

[From: Toro, GR, Silva, WJ, McGuire, RK and Herrmann, RB (1992) Probabilistic seismic hazard assessment of the Mississippi Embayment. *Seismological Research Letters* **63**(3), 449-475. Permission requested from SSA].